ISSN 1392–124X (print), ISSN 2335–884X (online) INFORMATION TECHNOLOGY AND CONTROL, 2015, T. 44, Nr. 4

# Adaptive Fuzzy Backstepping Control of MEMS Gyroscope Using Dynamic Sliding Mode Approach

**Yunmei Fang[1], Zhuli Yuan[2], Juntao Fei[3*]**

[1] *College of Mechanical and Electrical Engineering, Hohai University, Changzhou, 213022, China*

[2,3*] *College of IOT Engineering, Hohai University, Changzhou, 213022, China*
*e-mail: jtfei@yahoo.com*

crossref http://dx.doi.org/10.5755/j01.itc.44.4.9110

**Abstract**. In this paper, an adaptive fuzzy backstepping control using dynamic sliding mode control (AFBCDSMC) is presented for a micro-electromechanical system (MEMS) vibratory z-axis gyroscope. Based on an adaptive fuzzy backstepping control method, a dynamic sliding mode control is proposed to compensate and adjust the external disturbances and model uncertainties. The fuzzy control method with adaptive backstepping controller can approximate the system nonlinearities well without accurate system model and. It can make the controller have the ability to learn and adjust the fuzzy parameters in real time. In addition, dynamic sliding mode control can transfer discontinuous terms to the first-order derivative of the control input in order to effectively reduce the chattering. Simulation studies are investigated to demonstrate the satisfactory performance of the proposed method.

**Keywords**: dynamic sliding mode control; adaptive fuzzy backstepping control; MEMS gyroscope.

## 1. Introduction

Because of its advantages in the structure, volume and cost, MEMS gyroscope is widely used to measure the sensor angular velocity of inertial navigation and guidance system in aerospace, marine, aviation and positioning fields and land vehicle navigation. However, the presence of unavoidable errors in the design and manufacturing process, and the influence of the ambient temperature could decrease the accuracy and sensitivity of the gyroscope system. Therefore, how to compensate for manufacturing tolerances and accurate measurement of the angular velocity are the key issues of MEMS gyroscope. During the past years, a lot of control approaches have been applied to compensate and adjust the dynamic performance of the MEMS gyroscope.

Raman *et al.* [1] developed a closed-loop digitally controlled MEMS gyroscope with unconstrained sigma-delta force-feedback. Batur et al. [2] proposed a sliding mode controller of a simulated MEMS gyroscope. Dynamic sliding mode control has an excellent performance in reducing chattering since it can transfer the chattering in the control signal to its first derivative. Chen *et al.* [3] initiated an LTR-observer-based dynamic sliding mode control for chattering reduction. Koshkouei *et al.* [4] designed a novel dynamic sliding mode control for a dynamic system. Lin et al. [5] utilized a robust dynamic sliding mode control using adaptive RENN for magnetic levitation system. Shieh and Huang [6] proposed a trajectory tracking of piezoelectric positioning stages using a dynamic sliding-mode controller.

Adaptive fuzzy control is a powerful design tool for the dynamic system with parameters uncertainty and external disturbance. Hojati and Gazor [7] studied the hybrid adaptive fuzzy identification and control of nonlinear systems. Adaptive control algorithms for MEMS gyroscope [8-9] have been investigated because of their abilities to identify the parameters. Fei and Zhou [10] proposed a robust adaptive controller of MEMS triaxial gyroscope using fuzzy compensator. Hwang et al. [11] studied an adaptive fuzzy hierarchical sliding-mode control for the trajectory tracking of uncertain under actuated nonlinear dynamic systems. Lee [12] mainly studied a robust adaptive fuzzy control by backstepping for a class of MIMO nonlinear system. Adaptive backstepping sliding mode control approaches have been proposed for dynamic system such as leader-follower multi-agent systems and linear induction motor drive [13-14]. Lin and Li [15] designed a cascade adaptive fuzzy sliding mode controller for nonlinear two-axis inverted pendulum servomechanism. Adaptive fuzzy sliding controllers [16-18] received great interest in recent years because they do not depend on the system model and have great ability to learn and adjust the fuzzy parameters.

It is reasonable to combine the dynamic sliding mode control with adaptive fuzzy control and backstepping control for the control of MEMS gyroscope. In this paper, a dynamic sliding mode approach via adaptive fuzzy backstepping design is applied to realize the position tracking for the MEMS gyroscope. So far, to the best of authors' knowledge, it is the first time in the literature to use AFBCDSMC in MEMS gyroscope. The MEMS gyroscope model are transformed into cascade system which can be utilized in the backstepping design. The motivation of the proposed controller can be summarized as follows:

1) Backstepping design for a class of systems satisfying the strict feedback form can relax the matching condition appeared in the design of controller. The fuzzy control method combined with the adaptive backstepping control for MEMS gyroscope not only removes the requirements of accurate system model, but also obtains the self-learning ability and adjusts the fuzzy parameters. Therefore AFBCDSMC approach could attenuate the model uncertainties and external disturbances.

2) Adaptive control, fuzzy control, backstepping control and dynamic sliding mode control are combined and applied to MEMS gyroscope for the first time. Dynamic sliding mode control has high efficiency in solving the chattering problem. Hence, AFBCDSMC can not only provide improved tracking accuracy under sliding mode but also remove some of the fundamental limitations of the traditional approach.

3) The proposed backstepping dynamic sliding mode controller adds extra compensators for achieving and improving the system stability, hence obtaining desired system behavior and performance. Thus the entire closed-loop system can meet the expectations indicators of dynamic and static performance and achieve accurate position tracking performance.

This paper is structured as follows. In Section 2, the dynamic equation of MEMS vibratory gyroscope is established. In Section 3, a dynamic sliding mode controller via adaptive fuzzy backstepping method is derived to guarantee the asymptotic stability of the system. Simulation examples are shown in Section 4 to illustrate the excellent performance of the proposed AFBCDSMC. The conclusions are given in Section 5.

## 2. Dynamics of MEMS Gyroscope

Fig. 1 shows a typical $z$ axis MEMS vibratory gyroscope which includes a proof mass suspended by springs, an electrostatic actuation, and sensing mechanisms for forcing an oscillatory motion and sensing the position and velocity of the proof mass.

Assuming that the proof mass is mounted with a constant velocity, MEMS gyroscope is rotating at a constant angular velocity $\Omega_z$ over a sufficiently long time interval. The centrifugal forces $m\Omega_z^2 x$, $m\Omega_z^2 y$ are assumed to be negligible, MEMS gyroscope undergoes rotation about the $z$ axis only, and thereby Coriolis force is generated in a direction perpendicular to the drive and rotational axes.

Referring to [8] and using these assumptions, the dynamics of gyroscope can be derived as

$$\begin{aligned} m\ddot{x} + d_{xx}\dot{x} + d_{xy}\dot{y} + k_{xx}x + k_{xy}y &= u_x + 2m\Omega_z\dot{y} \\ m\ddot{y} + d_{xy}\dot{x} + d_{yy}\dot{y} + k_{xy}x + k_{yy}y &= u_y - 2m\Omega_z\dot{x} \end{aligned} \tag{1}$$

Fabrication imperfections contribute mainly to the asymmetric spring and damping terms, $k_{xy}$ and $d_{xy}$. The spring and damping terms of $x$ and $y$ axes, $k_{xx}$, $k_{yy}$, $d_{xx}$, and $d_{yy}$ are mostly known, but have small

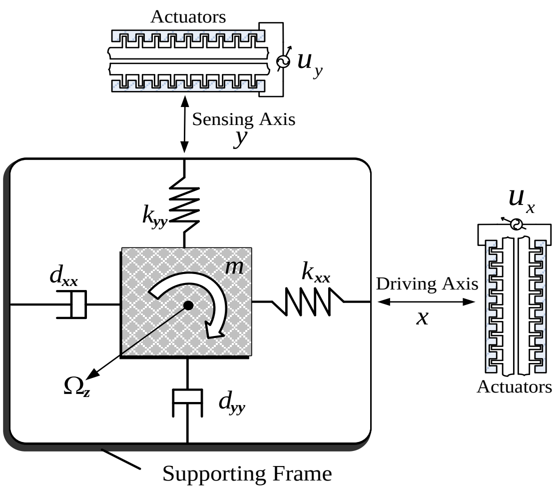


**Figure 1.** Schematic diagram of a MEMS gyroscope

unknown variations from their nominal values. The proof mass can be determined very accurately, and $u_x$, $u_y$ are the control forces in the $x$ and $y$ directions, respectively.

Dividing by the mass $m$, reference length $q_0$ and the square of the resonance frequency $w_0^2$ on both sides of Eq. (1), we can get

$$\frac{d_{xx}}{mw_0^2} \to D_{xx}, \frac{d_{xy}}{mw_0^2} \to D_{xy}, \frac{d_{yy}}{mw_0^2} \to D_{yy}, \frac{k_{xx}}{mw_0^2} \to w_x^2,$$

$$\frac{k_{xy}}{mw_0^2} \to w_{xy}, \frac{k_{yy}}{mw_0^2} \to w_y^2, \frac{\Omega_z}{w_0^2} \to \Omega_Z$$

Rewriting non-dimensional model (1) in vector form yields

$$\ddot{\mathbf{q}} + \mathbf{D}\dot{q} + \mathbf{K}\mathbf{q} = \mathbf{u} - 2\mathbf{\Omega}\dot{\mathbf{q}}, \tag{2}$$

where the dimensionless quantities of the expression are expressed as

$$\mathbf{q} = \begin{bmatrix} x \\ y \end{bmatrix}, \mathbf{D} = \begin{bmatrix} D_{xx} & D_{xy} \\ D_{xy} & D_{yy} \end{bmatrix}, \mathbf{K} = \begin{bmatrix} w_x^2 & w_{xy} \\ w_{xy} & w_y^2 \end{bmatrix},$$

$$\mathbf{u} = \begin{bmatrix} u_x \\ u_y \end{bmatrix}, \mathbf{\Omega} = \begin{bmatrix} 0 & -\Omega_Z \\ \Omega_Z & 0 \end{bmatrix}$$

By defining $\mathbf{x}_1 = \mathbf{q}, \mathbf{x}_2 = \dot{\mathbf{q}}$, MEMS gyroscope model (2) can be rewritten as

$$\begin{cases} \dot{\mathbf{x}}_1 = \mathbf{x}_2 \\ \dot{\mathbf{x}}_2 = -(\mathbf{D} + 2\mathbf{\Omega})\mathbf{x}_2 - \mathbf{K}_b\mathbf{x}_1 + \mathbf{u}. \end{cases} \tag{3}$$

Considering the model uncertainties and external disturbances, Eq. (3) can be expressed as

$$\begin{aligned} \dot{\mathbf{x}}_2 &= [-(\mathbf{D} + 2\mathbf{\Omega}) + \Delta\mathbf{A}_1]\mathbf{x}_2 \\ &\quad + (-\mathbf{K}_b + \Delta\mathbf{A}_2)\mathbf{x}_1 + (I + \Delta\mathbf{B})\mathbf{u} + \boldsymbol{\eta} \\ &= -(\mathbf{D} + 2\mathbf{\Omega})x_2 - \mathbf{K}_b\mathbf{x}_1 + \mathbf{u} + \mathbf{H}(t) \\ &= \mathbf{f}(x, y) + \mathbf{u} + \mathbf{H}(t), \end{aligned} \tag{4}$$

where $\Delta A_1, \Delta A_2, \Delta B$ are the uncertainties parts of dynamic model for MEMS gyroscope. $\boldsymbol{\eta}$ is the external disturbances of MEMS gyroscope.

$$\mathbf{f}(x, y) = -(\mathbf{D} + 2\mathbf{\Omega})x_2 - \mathbf{K}_b\mathbf{x}_1, \cdot$$

$$\mathbf{H}(t) = \Delta A_1\mathbf{x}_2 + \Delta A_2\mathbf{x}_1 + \Delta B\mathbf{u} + \boldsymbol{\eta}$$

including the model uncertainties and external disturbances in the MEMS gyroscope.

## 3. Dynamic Sliding Mode Control Using Adaptive Fuzzy Backstepping Controller

In this section, AFBCDSMC approach is designed to compensate and adjust the external disturbances and model uncertainties. The control target is to achieve the trajectory tracking of MEMS gyroscope. Fig. 2 shows the block diagram of AFBCDSMC for a MEMS gyroscope where the dynamic sliding controller and the adaptive fuzzy backstepping controller are derived. Suppose that the control objective is to make the trajectory of the MEMS gyroscopes follow the reference model and a reference trajectory is generated by an ideal oscillator.

The tracking error is defined as follows

$$\begin{cases} \mathbf{e}_1 = \mathbf{x}_1 - \mathbf{r} \\ \mathbf{e}_2 = \mathbf{x}_2 - \boldsymbol{\alpha} \end{cases} \tag{5}$$

where $r$ is a he reference input, $\boldsymbol{\alpha}$ is a virtual controller defined as

$$\boldsymbol{\alpha} = -c_1\mathbf{e}_1 + \dot{\mathbf{r}} \tag{6}$$

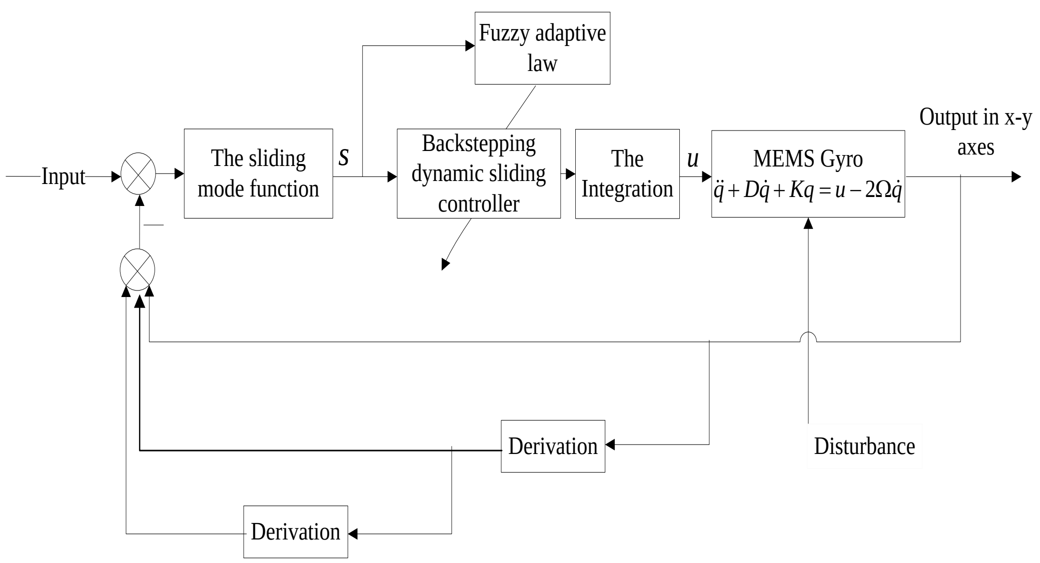


**Figure 2.** Block diagram of AFBCDSMC for a MEMS gyroscope

where the parameter $c_1$ of virtual controller satisfies the relationship $c_1 > 0$.

For the error equation (5), we define the first Lyapunov function candidate as :

$$V_1 = \frac{1}{2}\mathbf{e}_1^T\mathbf{e}_1 \tag{7}$$

The time derivative of $V_1$ is

$$\begin{aligned}\dot{V}_1 &= \mathbf{e}_1^T\dot{\mathbf{e}}_1 = \mathbf{e}_1^T(\mathbf{x}_2 - \dot{\mathbf{r}}) \\ &= \mathbf{e}_1^T(\mathbf{e}_2 - c_1\mathbf{e}_1) \\ &= -c_1\mathbf{e}_1^T\mathbf{e}_1 + \mathbf{e}_1^T\mathbf{e}_2\end{aligned} \tag{8}$$

Assuming $\mathbf{e}_2 = \mathbf{0}$, it is easy to see that the $\dot{V}_1 = -c_1\mathbf{e}_1^T\mathbf{e}_1 \le 0$, then the system is globally asymptotic stable and the error $\mathbf{e}_1$ asymptotically converges to zero.

The second Lyapunov function is selected as

$$V_2 = V_1 + \frac{1}{2}\mathbf{e}_2^T\mathbf{e}_2 + \frac{1}{2}\mathbf{s}^T\mathbf{s} \tag{9}$$

where $s$ is the function of sliding surface defined as

$$\begin{aligned}\mathbf{s} &= c\mathbf{e}_2 + \dot{\mathbf{e}}_2 \\ &= c\mathbf{e}_2 + \mathbf{f}(x, y) + \mathbf{u} + \mathbf{H}(t) - \boldsymbol{\alpha}\end{aligned} \tag{10}$$

where the parameter $c$ of sliding surface function is a positive constant.

From Eq.(4) and Eq.(10), we can get

$$\begin{aligned}\dot{\mathbf{x}}_2 &= \mathbf{f}(x, y) + \mathbf{s} - c\mathbf{e}_2 - \mathbf{f}(x, y) \\ &\quad -\mathbf{H}(t) + \dot{\boldsymbol{\alpha}} + \mathbf{H}(t) \\ &= \mathbf{s} - c\mathbf{e}_2 + \dot{\boldsymbol{\alpha}}.\end{aligned} \tag{11}$$

The time derivative of $\mathbf{s}$ is

$$\begin{aligned}\dot{\mathbf{s}} &= c\dot{\mathbf{e}}_2 + \dot{\mathbf{f}}(x, y) + \dot{\mathbf{u}} + \dot{\mathbf{H}}(t) - \ddot{\boldsymbol{\alpha}} \\ &= c(\dot{\mathbf{x}}_2 - \dot{\boldsymbol{\alpha}}) + \dot{\mathbf{f}}(x, y) + \dot{\mathbf{u}} + c_1\dot{\mathbf{x}}_2 - c_1\ddot{\mathbf{r}} - \dddot{\mathbf{r}} + \dot{\mathbf{H}}(t) \\ &= (c + c_1)\dot{\mathbf{x}}_2 - c\dot{\boldsymbol{\alpha}} + \dot{\mathbf{f}}(x, y) + \dot{\mathbf{u}} - c_1\ddot{\mathbf{r}} - \dddot{\mathbf{r}} + \dot{\mathbf{H}}(t).\end{aligned} \tag{12}$$

Substituting Eq. (11) into Eq. (12) yields

$$\begin{aligned}\dot{\mathbf{s}} &= (c + c_1)(\mathbf{s} - c\mathbf{e}_2) + c_1\dot{\boldsymbol{\alpha}} \\ &\quad + \dot{\mathbf{f}}(x, y) + \dot{\mathbf{u}} - c_1\ddot{\mathbf{r}} - \dddot{\mathbf{r}} + \dot{\mathbf{H}}(t).\end{aligned} \tag{13}$$

The time derivative of $V_2$ is:

$$\begin{aligned}\dot{V}_2 &= \dot{V}_1 + \mathbf{e}_2^T\dot{\mathbf{e}}_2 + \mathbf{s}^T\dot{\mathbf{s}} \\ &= -c_1\mathbf{e}_1^T\mathbf{e}_1 + \mathbf{e}_1^T\mathbf{e}_2 + \mathbf{e}_2^T(\dot{\mathbf{x}}_2 - \dot{\boldsymbol{\alpha}}) + \mathbf{s}^T[(c + c_1)(\mathbf{s} - c\mathbf{e}_2) \\ &\quad + c_1\dot{\boldsymbol{\alpha}} + \dot{\mathbf{f}}(x, y) + \dot{\mathbf{u}} - c_1\ddot{\mathbf{r}} - \dddot{\mathbf{r}} + \dot{\mathbf{H}}(t)] \\ &= -c_1\mathbf{e}_1^T\mathbf{e}_1 + \mathbf{e}_1^T\mathbf{e}_2 + \mathbf{e}_2^T(\mathbf{s} - c\mathbf{e}_2) + \mathbf{s}^T[(c + c_1)(\mathbf{s} - c\mathbf{e}_2) \\ &\quad + c_1\dot{\boldsymbol{\alpha}} + \dot{\mathbf{f}}(x, y) + \dot{\mathbf{u}} - c_1\ddot{\mathbf{r}} - \dddot{\mathbf{r}} + \dot{\mathbf{H}}(t)] \\ &= -c_1\mathbf{e}_1^T\mathbf{e}_1 + \mathbf{e}_1^T\mathbf{e}_2 - c\mathbf{e}_2^T\mathbf{e}_2 + \mathbf{s}^T[\mathbf{e}_2 + (c + c_1)(\mathbf{s} - c\mathbf{e}_2) \\ &\quad + c_1\dot{\boldsymbol{\alpha}} + \dot{\mathbf{f}}(x, y) + \dot{\mathbf{u}} - c_1\ddot{\mathbf{r}} - \dddot{\mathbf{r}} + \dot{\mathbf{H}}(t)].\end{aligned} \tag{14}$$

In the design of dynamic sliding mode controller, we choose exponential reaching law as

$$\dot{\mathbf{s}} = -k_1\,\text{sgn}(\mathbf{s}) - k_2\mathbf{s} \tag{15}$$

where the parameters $k_1$, $k_2$ of reaching law are positive constants.

In order to eliminate the related terms in Eq.(14), considering Eq.(15), we can design a dynamic sliding mode controller as

$$\begin{aligned}\dot{\mathbf{u}} &= -[\mathbf{e}_2 + (c + c_1)(\mathbf{s} - c\mathbf{e}_2) + c_1\dot{\boldsymbol{\alpha}} + \dot{\mathbf{f}}(x, y) - c_1\ddot{\mathbf{r}} - \dddot{\mathbf{r}} + \boldsymbol{\varphi}] \\ &\quad - \frac{\mathbf{s}}{\|\mathbf{s}\|^2}(\mathbf{e}_1^T\mathbf{e}_2 + k_3) - k_1\,\text{sgn}(\mathbf{s}) - k_2\mathbf{s}\end{aligned} \tag{16}$$

where the parameter $k_3$ is a positive constant.

Substituting Eq. (16) into Eq. (14) yields

$$\begin{aligned}\dot{V}_2 &= -c_1\mathbf{e}_1^T\mathbf{e}_1 - c\mathbf{e}_2^T\mathbf{e}_2 - k_1\mathbf{s}^T\,\text{sgn}(\mathbf{s}) \\ &\quad - k_2\mathbf{s}^T\mathbf{s} + \mathbf{s}^T(\dot{\mathbf{H}}(t) - \boldsymbol{\varphi}) - k_3,\end{aligned} \tag{17}$$

It can be observed from the expression of $\mathbf{H}(t)$ that it contains model uncertainties and external disturbances of MEMS gyroscope. Actually, $\mathbf{H}(t)$ is unknown in practical system, a fuzzy system is necessary to approximate $\dot{\mathbf{H}}(t)$. Through the reasoning algorithm of single value fuzzy, multiplied reasoning machine and center of gravity average defuzzification, a fuzzy system $\boldsymbol{\varphi}$ is used to approximate $\dot{\mathbf{H}}(t)$ which is a nonlinear function.

The ith fuzzy rule can be expressed as $R^i$ : If $x_i$ is $A_1^i$ and … $x_n$ is $A_n^i$, then $y$ is $y^i$, where $A_1^i, \ldots, A_n^i$ are fuzzy variables and $A_n^i$, $y^i$ are fuzzy sets.

So the output of the fuzzy system is

$$y = \frac{\sum_{i=1}^{N}\theta_i\prod_{j=1}^{n}\mu_{A_j^i}(x_j)}{\sum_{i=1}^{N}\prod_{j=1}^{n}\mu_{A_j^i}(x_j)} = \boldsymbol{\xi}^T\boldsymbol{\theta} \tag{18}$$

where $\mu_{A_j^i}(x_j)$ is membership function value of the fuzzy variable $x_j$, $\xi_i(x) = \frac{\prod_{j=1}^{n}\mu_{A_j^i}(x_j)}{\sum_{i=1}^{N}\prod_{j=1}^{n}\mu_{A_j^i}(x_j)}$,

$\boldsymbol{\xi} = [\xi_1(x) \quad \xi_2(x) \quad \ldots \quad \xi_N(x)]^T$ is fuzzy basis function vector, $\boldsymbol{\theta} = [\theta_1 \quad \theta_2 \quad \ldots \quad \theta_N]^T$, $N$ is the number of fuzzy rules.

For the fuzzy approximation of $\dot{\mathbf{H}}(t)$, $\varphi_1(x)$, $\varphi_2(x)$ are used to approximate $\dot{H}(1)$ and $\dot{H}(2)$ respectively in order to distinguish the model uncertainties and the external disturbances in $x$ axis from that in $y$ axis. The corresponding fuzzy system is designed as

$$\begin{cases} \varphi_1(x) = \dfrac{\sum_{i=1}^{N} \theta_{1i} \prod_{j=1}^{n} \mu_j^i(x_j)}{\sum_{i=1}^{N} \left[ \prod_{j=1}^{n} \mu_j^i(x_j) \right]} = \boldsymbol{\xi}_1^T(x)\boldsymbol{\theta}_1 \\ \varphi_2(x) = \dfrac{\sum_{i=1}^{N} \theta_{2i} \prod_{j=1}^{n} \mu_j^i(x_j)}{\sum_{i=1}^{N} \left[ \prod_{j=1}^{n} \mu_j^i(x_j) \right]} = \boldsymbol{\xi}_2^T(x)\boldsymbol{\theta}_2. \end{cases} \quad (19)$$

The fuzzy function is defined as

$$\boldsymbol{\varphi} = [\varphi_1 \quad \varphi_2]^T = \begin{bmatrix} \xi_1^T & 0 \\ 0 & \xi_2^T \end{bmatrix} \begin{bmatrix} \boldsymbol{\theta}_1 \\ \boldsymbol{\theta}_2 \end{bmatrix} = \boldsymbol{\xi}^T(x)\boldsymbol{\theta} \quad (20)$$

where $\boldsymbol{\xi}^T(x) = \begin{bmatrix} \xi_1^T & 0 \\ 0 & \xi_2^T \end{bmatrix}$, and $\boldsymbol{\theta} = \begin{bmatrix} \boldsymbol{\theta}_1 \\ \boldsymbol{\theta}_2 \end{bmatrix}$ is the adaptive fuzzy parameter.

We denote the optimal approximation constants by $\boldsymbol{\theta}^*$ and estimation error of the fuzzy parameters by $\tilde{\boldsymbol{\theta}} = \boldsymbol{\theta}^* - \boldsymbol{\theta}$. For a given small arbitrarily constant $\varepsilon(\varepsilon > 0)$, $\left\| \dot{\mathbf{H}}(t) - \boldsymbol{\xi}^T \boldsymbol{\theta}^* \right\| \le \varepsilon$ holds.

For the whole system, the third Lyapunov function is chosen as

$$V_3 = V_2 + \frac{1}{2}\tilde{\boldsymbol{\theta}}^T \tau^{-1} \tilde{\boldsymbol{\theta}} \quad (21)$$

where $\tau$ ($\tau > 0$) is an adaptive adjustable parameter.

The time derivative of $V_3$ is

$$\begin{aligned} \dot{V}_3 &= \dot{V}_2 - \tilde{\boldsymbol{\theta}}^T \tau^{-1} \dot{\boldsymbol{\theta}} \\ &= -c_1 \mathbf{e}_1^T \mathbf{e}_1 - c\mathbf{e}_2^T \mathbf{e}_2 - k_1 \mathbf{s}^T \operatorname{sgn}(\mathbf{s}) - k_2 \mathbf{s}^T \mathbf{s} \\ &\quad + \mathbf{s}^T (\dot{\mathbf{H}}(t) - \boldsymbol{\varphi}) - k_3 - \tilde{\boldsymbol{\theta}}^T \tau^{-1} \dot{\boldsymbol{\theta}} \\ &= -c_1 \mathbf{e}_1^T \mathbf{e}_1 - c\mathbf{e}_2^T \mathbf{e}_2 - k_1 \mathbf{s}^T \operatorname{sgn}(\mathbf{s}) - k_2 \mathbf{s}^T \mathbf{s} \\ &\quad + \mathbf{s}^T (\dot{\mathbf{H}}(t) - \boldsymbol{\xi}^T(x)\boldsymbol{\theta}) - k_3 - \tilde{\boldsymbol{\theta}}^T \tau^{-1} \dot{\boldsymbol{\theta}} \\ &= -c_1 \mathbf{e}_1^T \mathbf{e}_1 - c\mathbf{e}_2^T \mathbf{e}_2 - k_1 \mathbf{s}^T \operatorname{sgn}(\mathbf{s}) - k_2 \mathbf{s}^T \mathbf{s} \\ &\quad + \mathbf{s}^T (\dot{\mathbf{H}}(t) - \boldsymbol{\xi}^T(x)\boldsymbol{\theta}^*) + \mathbf{s}^T (\boldsymbol{\xi}^T(t)\boldsymbol{\theta}^* \\ &\quad - \boldsymbol{\xi}^T(t)\boldsymbol{\theta}) - k_3 - \tilde{\boldsymbol{\theta}}^T \tau^{-1} \dot{\boldsymbol{\theta}} \\ &= -c_1 \mathbf{e}_1^T \mathbf{e}_1 - c\mathbf{e}_2^T \mathbf{e}_2 - k_1 \mathbf{s}^T \operatorname{sgn}(\mathbf{s}) - k_2 \mathbf{s}^T \mathbf{s} \\ &\quad + \mathbf{s}^T (\dot{\mathbf{H}}(t) - \boldsymbol{\xi}^T(x)\boldsymbol{\theta}^*) + \mathbf{s}^T (\boldsymbol{\xi}^T(x)\tilde{\boldsymbol{\theta}}) - k_3 - \tilde{\boldsymbol{\theta}}^T \tau^{-1} \dot{\boldsymbol{\theta}} \\ &\le -c_1 \mathbf{e}_1^T \mathbf{e}_1 - c\mathbf{e}_2^T \mathbf{e}_2 - k_1 \mathbf{s}^T \operatorname{sgn}(\mathbf{s}) - k_2 \mathbf{s}^T \mathbf{s} \\ &\quad + \frac{1}{2}\|\mathbf{s}\|^2 + \frac{1}{2}\left\| \dot{\mathbf{H}}(t) - \boldsymbol{\xi}^T(x)\boldsymbol{\theta}^* \right\|^2 \\ &\quad - k_3 + \tilde{\boldsymbol{\theta}}^T [(\mathbf{s}^T \boldsymbol{\xi}^T(x))^T - \tau^{-1} \dot{\boldsymbol{\theta}}] \\ &\le -c_1 \mathbf{e}_1^T \mathbf{e}_1 - c\mathbf{e}_2^T \mathbf{e}_2 - k_1 \mathbf{s}^T \operatorname{sgn}(\mathbf{s}) - (k_2 - \frac{1}{2})\mathbf{s}^T \mathbf{s} \\ &\quad + \frac{1}{2}\varepsilon^2 - k_3 + \tilde{\boldsymbol{\theta}}^T [(\mathbf{s}^T \boldsymbol{\xi}^T(x))^T - \tau^{-1} \dot{\boldsymbol{\theta}}] \end{aligned} \quad (22)$$

To make $\dot{V}_3 \le 0$, the adaptive law is chosen as

$$\dot{\boldsymbol{\theta}} = \tau(\mathbf{s}^T \boldsymbol{\xi}^T(x))^T \quad (23)$$

Substituting Eq. (23) into Eq. (22) yields

$$\begin{aligned} \dot{V}_3 &\le -c_1 \mathbf{e}_1^T \mathbf{e}_1 - c\mathbf{e}_2^T \mathbf{e}_2 - k_1 \mathbf{s}^T \operatorname{sgn}(\mathbf{s}) \\ &\quad - (k_2 - \frac{1}{2})\mathbf{s}^T \mathbf{s} - \frac{1}{2}(2k_3 - \varepsilon^2) \end{aligned} \quad (24)$$

When parameters satisfy the condition of $k_2 \ge 1/2$, $2k_3 \ge \varepsilon^2$, the time derivatives meets $\dot{V}_3 \le 0$, so the third Lyapunov function $V_3$ is negative semi-definite. It ensures that $\mathbf{e}_1$, $\mathbf{e}_2$, $\mathbf{s}$, $\tilde{\boldsymbol{\theta}}$ are all bounded. According to Barbalat lemma, it can be proved that $\mathbf{s}(t)$ will asymptotically converge to zero, $\lim_{t\to\infty} \mathbf{s}(t) = 0$, from Eq. (10), $\mathbf{e}(t)$ also converges to zero asymptotically. Therefore asymptotic stability of the designed system using AFBCDSMC approach with can be guaranteed.

## 4. Simualtion Study

In this section, we will evaluate the proposed AFBCDSMC on the MEMS gyroscope model. The purpose of this controller is to reduce chattering and make the gyroscope system track the desired reference trajectory. The parameters of the MEMS gyroscope sensor are chosen as:

$$\begin{aligned} &\mathrm{m} = 1.8\times10^{-7} kg, k_{xx} = 63.955 N/m, \\ &k_{yy} = 95.92 N/m, k_{xy} = 12.779 N/m \\ &d_{xx} = 1.8\times10^{-6} N\cdot s/m, d_{yy} = 1.8\times10^{-6} N\cdot s/m, \\ &d_{xy} = 3.6\times10^{-7} N\cdot s/m \end{aligned}$$

The reference trajectory is selected as $r_1 = \sin(4.17t)$, $r_2 = 1.2\sin(5.11t)$, close to its natural frequencies in the x and y directions. The reference length $q_0$ is chosen as $q_0 = 1\mu m$ and the reference frequency $\omega_0$ is chosen as $w_0 = 1kHz$. Suppose that the input angular velocity is $\Omega_z = 100 rad/s$. Random variable signal with zero mean and unity variance are chosen as model uncertainties and external disturbance $\mathbf{H}(t)$.

Simulation study using AFBCDSMC is conducted. Initial conditions are $\mathbf{q}(0) = [0.2 \quad 0.2]^T$, other parameters are chosen as $c = 50$, $c_1 = 50$, $\tau = 40$, $k_1 = 20$, $k_2 = 100$, $k_3 = 200$. Gaussian membership function is chosen. Based on experience, combined with analysis and reasoning, the membership functions are selected as

$$\begin{aligned} &\mu_{F_i^1} = \exp[-0.5((x_i + A_i/2)/(A_i/4))^2], \\ &\mu_{F_i^2} = \exp[-0.5(x_i/(A_i/4))^2], \\ &\mu_{F_i^3} = \exp[-0.5((x_i - A_i/2)/(A_i/4))^2]. \end{aligned}$$

where $\mu_{F_i^j}$ is the membership function of $x_{F_i^j}$ ( $i=1,2,3,4,5$ ; $j=1,2,3$ ), $A_i$ is the amplitude of the reference trajectory, chosen as $\begin{bmatrix}1 & 1.2 & 4.17 & 6.132\end{bmatrix}$. $F_i^j$ are chosen as NB,NS,ZO, PS, PB, N stands for negative, P positive, B big, M medium, S small and ZO zero. The membership functions of the control system are shown in Fig. 3.

The simulation results are shown in Figures 4-9. Fig. 4 shows the actual output of MEMS gyroscope in $x, y$ axes. Fig. 5 depicts the tracking error between the actual output and the reference trajectory. It is shown that the trajectory of the control system can track the reference trajectory quickly. The control input using AFBCDSMC approach is displayed in Fig. 6. It is demonstrated that control input is smooth and stable in the region of -600 and 600.

Fig. 7 shows the derivative of control input. It can be observed from Figures 6-7 that the dynamic sliding mode controller is effective in obtaining a smooth control input by transferring chattering to its first order derivative. Figures 8 and 9 depicts the fuzzy adaptive parameters $\theta_1$ and $\theta_2$, illustrating that the fuzzy controller combined with adaptive control method can learn and adjust the fuzzy parameters adaptively. Therefore, the proposed AFBCDSMC approach for MEMS gyroscope can reduce the chattering and adapt to the changes of external disturbance and model parameters.

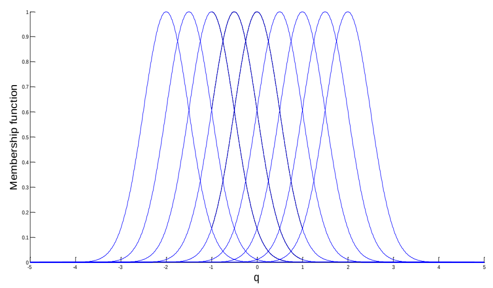


**Figure 3.** The membership functions

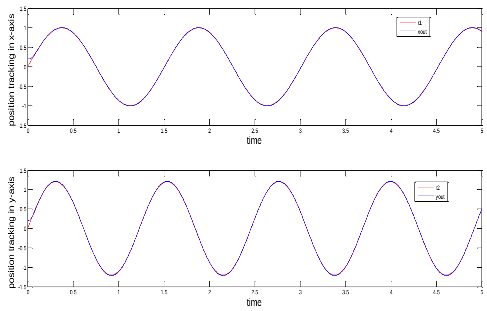


**Figure 4.** Trajectory tracking using AFBCDSMC approach

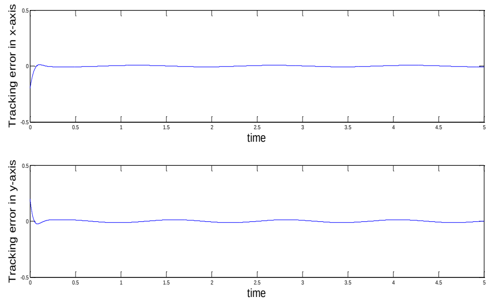


**Figure 5.** Tracking error using AFBCDSMC approach

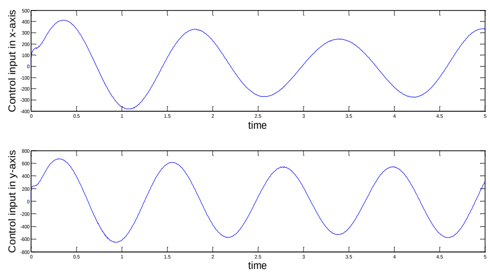


**Figure 6.** Control input using AFBCDSMC approach

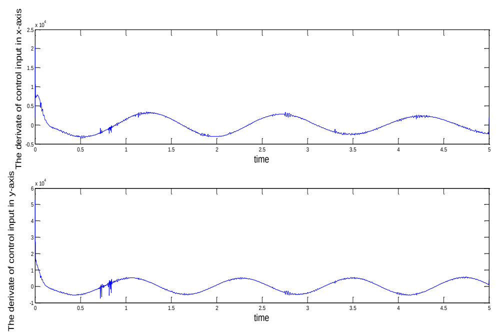


**Figure 7.** The derivative of control input using AFBCDSMC approach

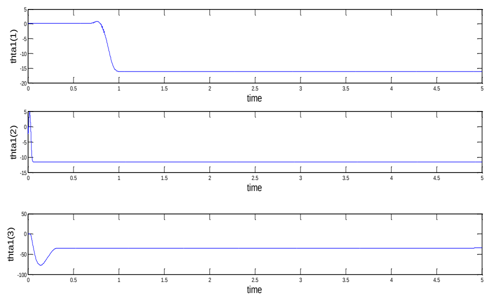


**Figure 8.** The fuzzy adaptive parameter $\theta_1$ using AFBCDSMC approach

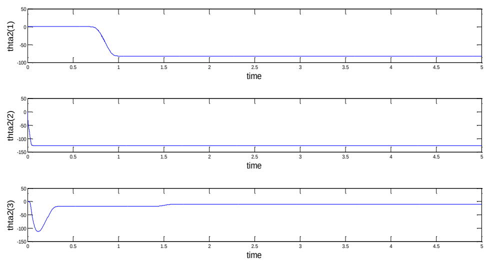


**Figure 9.** The fuzzy adaptive parameter $\theta_2$ using AFBCDSMC approach

## 5. Conclusions

In this paper, AFBCDSMC approach has been successfully applied to MEMS gyroscope through theoretical analysis and numerical simulation. The method AFBCDSMC can online adjust the fuzzy system parameters to approximate the dynamic model of MEMS gyroscope. The derivative switching function is employed to differentiate classical sliding surface and transfer discontinuous terms to the first-order derivative of the control input, thereby effectively reducing the chattering. Simulation studies are conducted to demonstrate the good performance of the proposed AFBCDSMC method in the presence of model uncertainties and external disturbances, showing the proposed method not only eliminates some of the fundamental limitations of the traditional sliding mode approach but also improves the tracking accuracy. In addition, the proposed approach can be extended to a general control system which can further demonstrate its potential in industry applications.

## Acknowledgments

We would like to present our thanks to anonymous reviewers for their helpful suggestions. This work is partially supported by National Science Foundation of China under Grant No. 61374100; Natural Science Foundation of Jiangsu Province under Grant No. BK20131136. The Fundamental Research Funds for the Central Universities under Grant No. 2014B04014.

## References

[1] **J. Raman, E. Cretu, P. Rombouts, L. Weyten.** A closed-loop digitally controlled MEMS gyroscope with unconstrained sigma-delta force-feedback. *IEEE Sensors Journal*, 2009, Vol. 9, No.3, 297-305.

[2] **C. Batur, T. Sreeramreddy, Q. Khasawneh.** Sliding mode control of a simulated MEMS gyroscope, *ISA Transactions*, 2006, Vol. 45, No. 1, 99-108.

[3] **M. Chen, C. Chen, F. Yang.** An LTR-observer-based dynamic sliding mode control for chattering reduction, *Automatica*, 2007, Vol. 43, No. 6, 1111-1116.

[4] **A. Koshkouei, K. Burnham, A. Zinober.** Dynamic sliding mode control design. *IEE Proceedings-Control Theory and Applications*, 2005, Vol. 152, No. 4, 392–396.

[5] **F. Lin, S. Chen, K. Shyu.** Robust dynamic sliding-mode control using adaptive RENN for magnetic levitation system. *IEEE Trans. on Neural Networks*, 2009, Vol. 20, No. 6, 938-951.

[6] **H. Shieh, P. Huang.** Trajectory tracking of piezoelectric positioning stages using a dynamic sliding-mode control. *IEEE Trans. on Ultrasonics, Ferroelectrics and Frequency Control*, 2006, Vol. 53, No. 10, 1872–1882.

[7] **M. Hojati, S. Gazor.** Hybrid adaptive fuzzy identification and control of nonlinear systems. *IEEE Trans. on Fuzzy Systems*, 2002, Vol. 10, No. 2, 198-210.

[8] **J. Fei, C. Batur.** A novel adaptive sliding mode control with application to MEMS gyroscope. *ISA Tranactions*, 2009, Vol. 48, No. 1, 73-78.

[9] **R. Leland.** Adaptive control of a MEMS gyroscope using Lyapunov methods. *IEEE Trans. on Control Systems Technology*, 2006, Vol. 14, No. 2, 278-283.

[10] **J. Fei, J. Zhou.** Robust adaptive control of MEMS triaxial gyroscope using fuzzy compensator, *IEEE Trans. on Systems, Man, and Cybernetics, Part B: Cybernetics*, 2012, Vol. 42, No. 6, pp. 1599-1607.

[11] **C. Hwang, C. Chiang, Y. Yeh.** Adaptive fuzzy hierarchical sliding-mode control for the trajectory tracking of uncertain underactuated nonlinear dynamic systems. *IEEE Trans. on Fuzzy Systems*, 2014, Vol. 22, No. 2, 286-299.

[12] **H. Lee.** Robust adaptive fuzzy control by backstepping for a class of MIMO nonlinear systems. *IEEE Trans. on Fuzzy Systems*, 2011, Vol. 19, No. 2, 265-275.

[13] **D. Zhao, T. Zou, S. Li, Q. Zhu.** Adaptive back-stepping sliding mode control for leader-follower multi-agent systems. *IET Control Theory & Applications*, 2012, Vol. 6, No. 8, 1109-1117.

[14] **F. Lin, P. Shen, P. Hsu.** Adaptive backstepping sliding mode control for linear induction motor drive. *IEE Proceedings-Electric Power Application*, 2002, Vol. 149, No. 3, 184-194.

[15] **C. Lin, H. Li.** TSK fuzzy CMAC-based robust adaptive backstepping control for uncertain nonlinear systems. *IEEE Trans. on Fuzzy Systems*, 2012, Vol. 20, No. 6, 1147-1154.

[16] **R. Wai, M. Kuo, J. Lee.** Design of cascade adaptive fuzzy sliding-mode control for nonlinear two-axis inverted-pendulum servomechanism. *IEEE Trans. on Fuzzy Systems*, 2008, Vol. 16, No. 5, 1232-1244.

[17] **C. Lin, C. Hsu.** Adaptive fuzzy sliding-mode control for induction servomotor systems. *IEEE Trans. on Energy Conversion*, 2004, Vol. 19, No. 2, 362-368.

[18] **T. Ho, K. Ahn.** Speed control of a hydraulic pressure coupling drive using an adaptive fuzzy sliding-mode control. *IEEE/ASME Trans. on Mechatronics*, 2012, Vol. 17, No. 5, 976-986.

Received January 2015.